CHROM. 11,728

MASS TRANSFER IN IDEAL AND GEOMETRICALLY DEFORMED OPEN TUBES

I[*]. IDEAL AND COILED TUBES WITH CIRCULAR CROSS-SECTION[**]

KURT HOFMANN and ISTVÁN HALÁSZ

Angewandte Physikalische Chemie, Universität des Saarlandes, 6600 Saarbrücken (G.F.R.)

(Received August 16th, 1978)

SUMMARY

A summary of the hydrodynamics relevant to open tubes is presented. The band broadening of unretained samples in ideal and coiled tubes with circular cross-sections (0.25–4 mm I.D.) was measured with *n*-heptane and water as eluents. The lack of any appreciable interference from instrumental factors is substantiated by the experimentally determined diffusion coefficients and critical Reynold's numbers. It is shown that carefully prepared copper tubes behave as ideally as the corresponding glass tubes. With decreasing tube diameter, wall roughness leads to greater radial mass transfer. This effect is evident in 0.25-mm I.D. copper tubes and 0.5-mm (or even 0.75-mm) I.D. stainless-steel tubes, and can be used to advantage in constructing heat exchangers, connecting tubes or reaction detectors in liquid chromatography.

It is shown for the first time that the onset of turbulence can be detected with considerably higher sensitivity by means of *h* versus *u* curves than by the *K* versus *u* curves used previously.

It is shown that at the onset of turbulence the specific permeability decreases by a factor of about 3. Band broadening in the turbulent region was found to be ten times greater than that calculated on the basis of the friction theory of Taylor, apparently because laminar conditions prevail in a substantial portion of the tube cross-section.

If an ideal tube is coiled, its specific permeability decreases with increasing velocity. Furthermore, coiling stabilizes "laminar" flow and the beginning of the turbulent region is shifted to higher Reynold's number (*i.e.*, higher velocities).

It is shown that, as the inner diameter of the open tube decreases, higher linear velocities are required in order to decrease band broadening substantially (*e.g.*, by a factor of 5) for coiled tubes than for ideal tubes. For example, a linear velocity of 250 cm/sec is necessary to achieve this factor of 5 with 0.25-mm I.D. tubing, even though the presence of secondary flow is indicated by the *K* versus *u* curve at *u* > 10 cm/ sec. For liquid chromatographic separations tubes narrower than 0.25 mm I.D. are essential. Therefore, at acceptable linear velocities (<50 cm/sec), the coiling of an

ideal tube will not reduce band broadening appreciably in comparison with that in straight (ideal) tubes.

Secondary flow effects at high velocities, however, may decrease the h values markedly. The h value in a coiled tube of 1.2 mm I.D. was 290 times smaller at $u = 250$ cm/sec than in a corresponding ideal tube.

INTRODUCTION

In gas chromatography, the principal advantage of open tubes (capillary columns) over packed columns lies in the considerably greater number of theoretical plates (n) that can be generated per unit pressure drop[1]. In liquids the diffusion coefficients are about 10^4 times smaller than in gases, which results in greater band broadening in liquid mobile phases. Further, the ca. 100-fold higher viscosity of liquids compared with gases requires a greater pressure drop over the column to achieve the same linear velocities for similar tube geometries. Consequently, efforts have constantly been made to apply the advantages of open tubes to high-performance liquid chromatography (HPLC).

This paper compares the behaviour of ideal open tubes in the region of laminar and turbulent flow and discusses the radial mass transfer within them. In Part II, potential applications of ideal and coiled open tubes in liquid chromatography are discussed. Part II also describes the advantages of other types of geometrically deformed tubes[2-11], which stem primarily from the more rapid radial mass transfer within them. This is not only essential in liquid chromatography, but is also desirable for heat exchangers[8], mixing tubes (including reaction detectors), and connecting tubing between the sampling device and the column and between the column and the detector in HPLC.

In classical hydrodynamics, the various types of flow (e.g., laminar and turbulent) are described in terms of the specific permeability, K, (which will be abbreviated to permeability) as a function of the cross-sectionally averaged linear velocity, u. It will be shown that the relative band broadening, h, (also called the height equivalent to a theoretical plate) is a more sensitive function of the type of flow than the permeability. Therefore, the ordinary chromatographic method may be very useful in hydrodynamics.

This paper describes only the properties of inert samples ($k' = 0$), as band spreading can only increase with increasing capacity ratios, k'.

As chromatographers are not always conversant with the basic principles of hydrodynamics, a brief description will be presented first. It will be demonstrated by measurements in ideal tubes that no additional band broadening accrues from the apparatus. Finally, the hydrodynamic properties of geometrically deformed tubes (coiled, squeezed, twisted and undulated) fabricated from various column materials (glass, copper, stainless steel, aluminium and Teflon) will be described.

FUNDAMENTAL PRINCIPLES OF HYDRODYNAMICS

In this summary, the usual detailed and thorough treatment of hydrodynamics will be dispensed with.

Liquid flow in ideal tubes

Ideal open tubes are straight tubes with a constant circular cross-section, a smooth inner wall and smooth inlet and outlet surfaces. The tube must be long enough that disturbances at the inlet and outlet are negligibly small.

The compressibility of liquids[12] will always be neglected.

For laminar flow in ideal tubes, it will be assumed that:

(a) there are co-axial layers in the flowing medium where the velocity is constant;

(b) except for diffusion flow, no radial flow takes place;

(c) the cross-sectionally averaged linear velocity can be described by means of the Hagen–Poiseuille equation[13,14]:

$$u = \frac{K \, \Delta P}{\eta \, L} = \frac{r^2 \, \Delta P}{8\eta \, L} \tag{1}$$

(see list of symbols at the end of the paper);

(d) the maximum linear velocity at the centre of the tube is

$$u_{max} = 2\,u \tag{2}$$

(e) for "real" tubes the length of the inlet disturbance, L_e, (ref. 15) is given by

$$L_e = 100\,d = 200\,r \tag{3}$$

(f) the Reynold's number, Re, is less than 2000–2300, where

$$Re = \frac{\varrho d u}{\eta} = \frac{2ru}{\nu} \tag{4}$$

(g) the permeability, K, is not a function of the linear velocity;

(h) the wall of the tube is inert, *i.e.*, there is no interaction between the wall and the liquid phase.

Mass transfer processes in ideal tubes

As shown by Taylor[16], dispersion in flowing liquids is not an isotropic property. Aris[17] extended the theory of Taylor to include axial diffusion for dispersion in flowing liquids and gave the dynamic diffusion coefficient as

$$D_{dyn} = D + \frac{r^2 u^2}{48D} \tag{5}$$

Based on additional conclusions of Aris, D_{dyn} may be substituted in the unidimensional Einstein diffusion equation[18]:

$$\sigma^2 = 2D_{dyn}t \tag{6}$$

and rewritten[5] in chromatographic nomenclature as

$$h \equiv \frac{\sigma^2}{L} = \frac{2D}{u} + \frac{r^2 u}{24D} \tag{7}$$

For $u > 0.01$ cm/sec, the first term on the right-hand side of eqn. 7 becomes negligible for liquids (this is identical with the approach of Taylor), and thus the Aris theory to a good approximation can be written as

$$h = \frac{r^2 u}{24D} \tag{8}$$

Golay[1] extended the Aris theory to include mass transfer at non-inert tube walls. It should be noted here that the Golay equation is not valid even for coiled tubes, let alone geometrically deformed tubes.

Turbulent flow in ideal tubes

To a first approximation, if $Re > 2300$ the flow becomes turbulent. With the onset of turbulence a substantial distortion of the flow profile[15,19] occurs, in relation to laminar flow. As a result of the radial flow that appears on reaching turbulence,

$$u_{max} = 1.22u \tag{9}$$

For turbulent flow the length of the inlet or outlet disturbance is

$$L_e = 40d \tag{10}$$

Formally, eqn. 1 can also be applied to the turbulent region by taking into account that K decreases monotonically with increasing flow-rate, as will be shown experimentally. In the transition region from laminar to turbulent flow the permeability decreases sharply at first and then more gradually. The theory of turbulent flow[11] will not be discussed here, as it is beyond the scope of this paper.

In chromatographic discussions, it has frequently been suggested that operation in the turbulent region should optimize dispersion and mass transfer both for gas[2] and liquid chromatography. However, it is sometimes overlooked that the high velocities and lower (poorer) permeabilities necessitate a higher pressure drop over the column by up to a factor of 3. This aggravates almost all instrumental problems. It is also open to question whether the rate of mass transfer in (or on) the stationary phase can keep up with this high linear velocity of the mobile phase. At such high velocities, the risk of mechanical erosion should not be underestimated.

Liquid flow in coiled tubes with a circular cross-section

In coiled tubes with a circular cross-section, a radial mixing flow occurs, which is called secondary flow[20,21]. This secondary flow is caused by the centrifugal forces, f. These forces can be related to the volume element, V, for convenience and can be described by

$$\frac{f}{V} = \frac{\varrho u^2}{R} \tag{11}$$

where ϱ is the density of the flowing medium and R the distance from the tube axis. This disrupts the flow profile to the extent that the radial mixing equalizes the velocity differences to a certain extent. This radial mass transport is desirable for chromatography and heat exchangers. Whenever secondary flow occurs, the permeability becomes a monotonically decreasing function of the flow-rate even in the "laminar" region ($Re < 2300$) and the onset of turbulence is displaced to greater Reynold's numbers.

Coiling produces the least geometric change in ideal tubes, but it is then no longer possible to give an explicit mathematical description of the flow profile or of the mass transfer phenomena. These problems become even more difficult for more complex geometric forms such as oval cross-sections (squeezed) and/or twisted shapes. In such instances only the experimental results can be presented, systematically if possible.

EXPERIMENTAL

Chromatographic equipment

The measurements were performed with a home-made apparatus[11,22,23]. A piston diaphragm pump (Orlita, Giessen, G.F.R., Type S 15) was used to provide a pulseless[23] flow of eluent. The sampling device[22] and the home-made UV detector (254 nm) were adapted to the tubes[11], so that the inlet and outlet disturbances were negligible. The dead volumes of the apparatus were minimized and the detector response times were optimized to measure real phenomena within the limits of error given.

Preparation of glass tubes

A sophisticated apparatus was developed[11] by means of which even glass tubes with an oval cross-section could be twisted reproducibly and coiled.

Treatment of metal tubes

The metal tubes were rinsed with methylene chloride before use. In order to smooth and harden the material (copper), the straight tubes, before being stretched, were carefully coiled around a *ca.* 11-cm diameter cylinder under a light tensile strain. Any residual ripples in the tubes were negligible, as evidenced by the fact that essentially literature values were measured for Re_{crit} and D. The copper capillary and stainless-steel tubing with more or less smooth inner surfaces were obtained from Schoeller (Hellenthal/Eifel, G.F.R.) and the aluminium tubing with a smooth inner surface from Cochius (Frankfurt/Main, G.F.R.).

Mobile phases and samples

The following eluent/sample systems were used: (a) *n*-heptane/1 vol.-% benzene in *n*-heptane; (b) methylene chloride/1 vol.-% benzene in methylene chloride; and (c) water/5 vol.-% acetone in water.

The amounts of sample varied between 2 and 10 μl, depending on the tube diameter. All measurements were carried out at room temperature.

For the calculation of Reynold's numbers, the following values were used:

	Density (g/cm³)	Dynamic viscosity (Poise)	Kinematic viscosity (Stokes)
n-Heptane	0.68	$4 \cdot 10^{-3}$	$5.9 \cdot 10^{-3}$
Water	1.0	$10 \cdot 10^{-3}$	$10 \cdot 10^{-3}$

Evaluation of the chromatograms

The relative band broadening (h values) was calculated by means of the equation

$$h = \frac{Lw^2}{16t_0^2} \tag{12}$$

The h values were usually reproducible to better than $\pm 5\%$.

The permeability, K, of the tubes was calculated by means of eqn. 1. Manometers of grade 1.0 were used. Except for unusually difficult cases, the accuracy of these measurements was better than $\pm 10\%$. The determination of the centre of mass of some peaks with ideal tubes was particularly difficult.

MEASUREMENTS WITH IDEAL TUBES

n-Heptane as mobile phase

Most measurements were carried out with 10-m tubes. As will be shown, the pre-treated copper usually behaved ideally and therefore no measurements with glass tubes are described here.

In the following sections, typical experimental results will first be discussed in detail for the 1-mm I.D. tubing. All other results, for tubing between 0.25 and 4 mm I.D., will be presented subsequently in order of increasing diameters.

Fig. 1 shows the permeability, K, of an ideal copper tube (1 mm I.D. × 2 mm O.D.) as a function of the cross-sectionally averaged linear velocity, u. The turbulent region ($Re = 2040$) was attained at $u_{crit} = 120$ cm/sec. The K values in the laminar

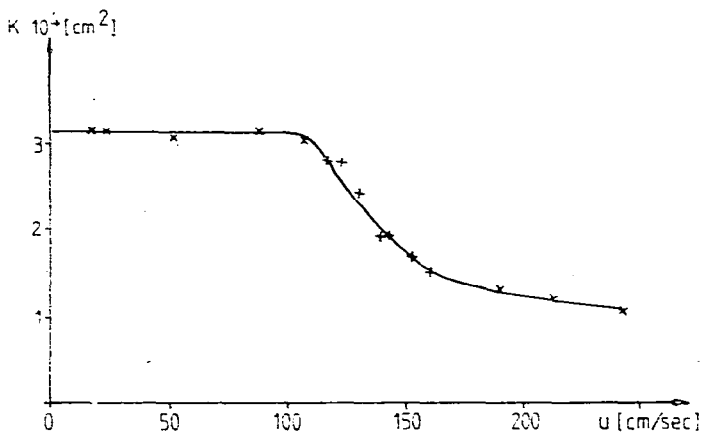Fig. 1. K versus u curve for an ideal open tube (I.D. 1 mm). Copper tube (1.0 mm I.D. × 2.0 mm O.D.), $L = 10$ m. Eluent, n-heptane; sample, benzene; room temperature.
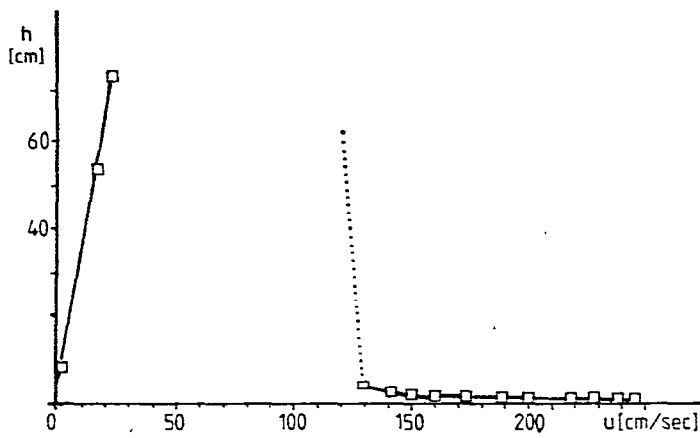
Fig. 2. h versus u curve for an ideal open tube. Conditions as in Fig. 1.

region correspond to those calculated via eqn. 1 ($K_{theo} = 3.1 \cdot 10^{-4}$ cm^2). When u was increased to 2 u_{crit} (240 cm/sec) the permeability deteriorated by a factor of 3. The experimental scatter shown in Fig. 1 is characteristic of the accuracy attainable with ideal tubes.

Fig. 2. depicts the h versus u plot for the same copper tube. In the laminar region, even careful and rapid sample application yielded asymmetric peaks if the residence time, t, in the tube was not long enough. As can be seen, the h values could be calculated if $u < 30$ cm/sec ($t > 33$ sec). In this region, the experimental h values agree with those calculated from the Taylor approximation (eqn. 8). In the laminar region with $30 < u < 120$ cm/sec the peaks were asymmetric and therefore could not be evaluated (dotted line in Fig. 2). At higher velocities the dotted line shows the calculated (eqn. 8) h values. In the turbulent region ($u > 120$ cm/sec), very symmetrical peaks were obtained. At $u = 130$ cm/sec the relative band broadening decreased abruptly ($h = 2.5$ cm) and continued to diminish slowly with increasing u. As later measurements showed, and as has already been pointed out earlier[5], an h versus u plot is a substantially more sensitive indicator of the type of flow of a liquid than is the hydrodynamic quantity K.

Measurements similar to those discussed above were carried out at room temperature with 10 m $\times$ 0.5–2-mm I.D. copper tubes. The results are summarized in

TABLE I

EXPERIMENTAL PARAMETERS DETERMINED IN IDEAL OPEN TUBES

Eluent, n-heptane; sample, benzene; room temperature.

I.D. $\times$ O.D. of tube (mm)	u_{sym} (cm/sec)	u_{turb} (cm/sec)	h_{turb} (cm)	$D_{calc} \cdot 10^5$ (cm^2/sec)
0.5 $\times$ 1.5	78	230	2.3	3.3
0.75 $\times$ 2.0	35	170	2.2	3.4
1.0 $\times$ 2.0	25	130	2.0	3.4
1.2 $\times$ 2.0	20	115	2.5	3.4
1.4 $\times$ 2.0	15	90	3.0	3.6
2.0 $\times$ 4.0	6.4	60	3.0	4.1

Table I. The first column lists the inner or outer diameter of the tube. The second column (u_{sym}) indicates the maximum linear velocity at which symmetrical peaks are still obtained and at which the rise of the h versus u curve is linear. The next two columns (u_{turb} and h_{turb}) give the velocity and the relative band broadening at incipient turbulence, respectively. It is noteworthy that the onset of turbulence was almost always manifest at lower velocities in h versus u curves than in K versus u plots, even though the velocity differences were within the probable error limits (*ca.* 5–10%). The calculated diffusion coefficients, D_{calc}, of benzene in *n*-heptane (last column) will be discussed later. In this study the onset of turbulence occurred between Reynold's numbers of 2040 and 2160.

The data in Table I substantiate that the apparatus had been carefully constructed and that the inlet and outlet disturbances, with exception of the last row of results, were negligible.

In contrast to the tubes evaluated in Table I, the roughness in 0.25 mm I.D. × 1.5 mm O.D. tubes was not negligible (Fig. 3). The h versus u curve is linear up to $u = 70$ cm/sec, then flattens out, passes through a maximum and declines sharply. The measurements were extended to $u = 515$ cm/sec, the onset of turbulence ($Re = 2180$). However, complete turbulence could not be achieved, as is evident from the h versus u curve. In "rough-walled" small-diameter tubes, the transition from laminar to turbulent flow appears to take place continuously.
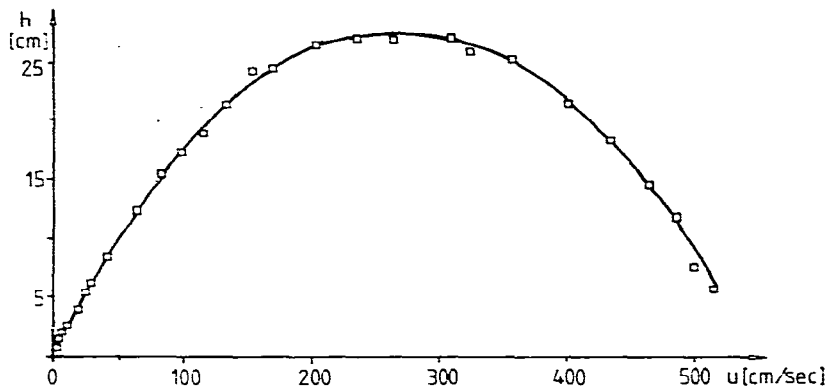

Fig. 3. h versus u curve for an open tube (I.D. 0.25 mm) with wall roughness. Conditions as in Fig. 1, except 0.25 mm I.D. × 1.5 mm O.D.

It should be noted that the degree of unevenness of the inner wall of the copper tubing was independent of the diameter. Hence, the smaller the inner diameter, the greater is the effect of the roughness, as can be seen from Table I and Fig. 3. This effect is considerably more pronounced with stainless-steel tubes. A small inner diameter and a rough wall destroy the classic laminar flow and enhance radial mass transfer. Such tubes are to be preferred as connecting tubing for liquid chromatographic equipment and heat exchangers. However, with decreasing diameter clogging of these tubes becomes more likely, especially if they are connected after a packed column where particles may be discharged.

Band broadening in the turbulent region of open tubes. The friction theory of turbulent flow[24] was used by Taylor to calculate dispersion in tubes in that region for

the first time. It is postulated that radial fluctuations extending to the tube wall are superimposed on the axial flow of liquid. A calculation based on this friction theory yields $h = 7.4 \cdot 10^{-2}$ cm for a 1-mm I.D. tube and an eluent velocity of $u = 176$ cm/ sec ($Re = 3000$) (p. 45 in ref. 11). The experimental h value in Fig. 2, however, is at least 10 times greater. This discrepancy can be explained by the Prandtl boundary layer theory of turbulent flow [19,25,26]. Based on our experimental results, up to 20% of the cross-section of a "turbulent" flow consists of a laminar layer flow. In other words, in the turbulent region the experimentally determined dispersion is at least 10 times that calculated from the friction theory.

   Determination of diffusion coefficients (D) in ideal tubes. The diffusion coefficient of a substance in a particular eluent can be determined from the ascending portion of an *h versus u* curve with the aid of eqn. 8. As can be seen from the first five values in the last column in Table I, the D_{calc} value for benzene in *n*-heptane is calculated to be $3.3 \cdot 10^{-5}$–$3.6 \cdot 10^{-5}$ cm²/sec at room temperature. These values are based on the low sample concentrations (< 100 ppm) encountered in open chromatographic columns. A value of $D = 3.7 \cdot 10^{-5}$ cm²/sec is calculated for this system from the Wilke–Chang equation[27]. Such excellent agreement must be regarded as fortuitous, but it nevertheless does indicate that mechanical mixing (due to inlet turbulence, wall roughness, etc.) was negligible in the copper tubes used.

Water as mobile phase

   Water was selected as the second mobile phase because its kinematic viscosity, ν, is about double that of *n*-heptane and because it is frequently employed in chromatography. The dispersion properties of acetone (as sample) in water were determined in all of the copper tubes described in the previous section. The inner diameters of the tube calculated using eqn. 1 were independent of whether water or *n*-heptane was the eluent. The shapes of the *h versus u* curves for water were similar to those obtained for *n*-heptane (Fig. 2). The most important experimental results are summarized in Table II.

TABLE II

EXPERIMENTAL PARAMETERS DETERMINED IN IDEAL OPEN TUBES

Eluent, water; sample, acetone; room temperature.

I.D. × O.D. of tube (mm)	u_{sym} (cm/sec)	u_{turb} (cm/sec)	h_{turb} (cm)	$D_{calc} \cdot 10^5$ (cm²/sec)
0.5 × 1.5	20	330	5.3	1.1
0.75 × 2.0	16	280	2.5	1.3
1.0 × 2.0	8	222	2.0	1.4
1.2 × 2.0	8	170	4.0	1.3
1.4 × 2.0	8	167	5.0	2.6

   Because of the higher kinematic viscosity of water, u_{sym} is smaller than with *n*-heptane. However, u_{sym} is not strictly proportional to D. Before complete turbulence is reached, the peaks are symmetrical and the *h* values decrease very steeply with increasing velocity, as a result of which the determination of u_{turb} and h_{turb} is imprecise. The same is true of the measurements of u_{sym}. The diffusion coefficient of acetone in water was calculated to be $1.1 \cdot 10^{-5}$–$1.4 \cdot 10^{-5}$ cm²/sec.

The roughness of the wall of the 0.25 mm I.D. × 1.5 mm O.D. copper tubing was also noticeable in this instance. The turbulent region with water could not be attained because the pressure drop of about 500 atm required to achieve $u = 800$ cm/sec was not compatible with the sampling device used. As shown in Fig. 4, h rises linearly to $u = 40$ cm/sec and then increases more slowly until a plateau of $h \approx 60$ cm is reached. Particularly noteworthy is the large experimental scatter when $u > 160$ cm/sec, which is greater than the experimental uncertainty. When the wall roughness is not negligible, characteristic curves are obtained such as those shown in Fig. 4.

The inlet and outlet disturbances in 1.4 mm I.D. × 2.0 mm O.D. tubes also led to excessively high calculated diffusion coefficients, as shown in Table II.
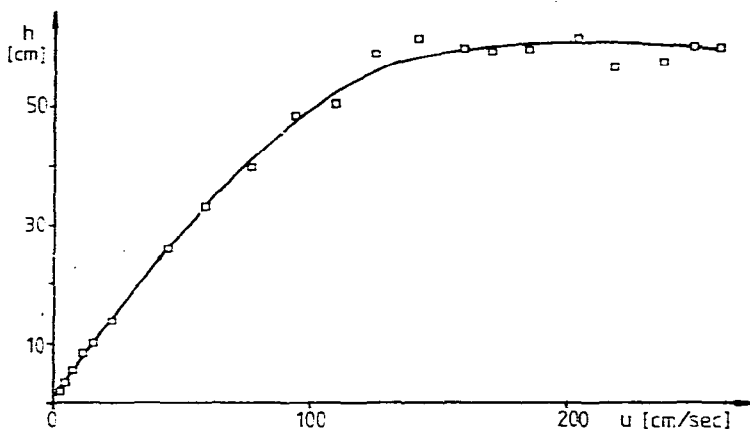
Fig. 4. *h versus u* curve for an open tube (I.D. 0.25 mm) with wall roughness. Copper tube (0.25 mm I.D. × 1.5 mm O.D.), $L = 10$ m. Eluent, water; sample, acetone; room temperature.

MEASUREMENTS ON COILED TUBES WITH A CIRCULAR CROSS-SECTION

n-Heptane as mobile phase

In order to simplify the comparison between the flow properties of ideal and coiled tubes, the lengths and inner diameters of the copper tubes were kept constant and the measurements were carried out with *n*-heptane as mobile phase and benzene as sample. Unless stated otherwise, the coil diameter was always 12 cm.

Fig. 5 depicts the permeability as a function of the velocity in a 1.0 mm I.D. × 2.0 mm O.D. coiled copper tube (solid line). For comparison, the data for the corresponding ideal tube, which have already been presented in Fig. 1, are included (broken line).

As can be seen from Fig. 5, the permeabilities of the ideal and coiled tubes coincide only at very low velocities. The permeability of the coiled tubes decreases steadily with increasing u and continues thus into the turbulent region of the ideal tube. For liquid flow in coiled tubes, the critical velocity corresponding to the onset of turbulent flow can no longer be determined accurately.

Fig. 6 shows that the dispersion in the coiled tube is greatly reduced as a result of the secondary flow. The difficulties with sample introduction in the case of
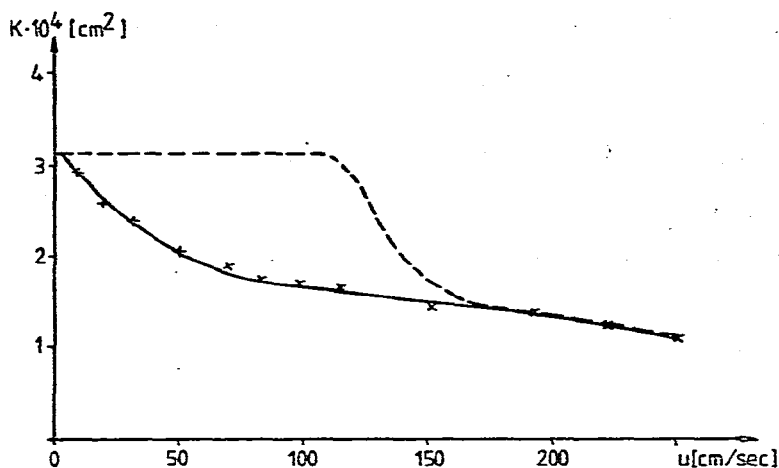
Fig. 5. K versus u curve for a coiled tube (I.D. 1 mm). Copper tube (1.0 mm I.D. × 2.0 mm O.D.), $L = 10$ m. Coil diameter: 12 cm. Eluent, n-heptane; sample, benzene; room temperature. Solid line, coiled tube; broken line, ideal tube.

the ideal tube, *i.e.*, peaks that cannot be evaluated (Fig. 2), are absent here as a result of the extensive mixing created by the secondary flow. However, the experimental scatter in the velocity range 30–120 cm/sec is greater than for the ideal tubes.

Turbulence in coiled tubes appears later ($Re = 2900$, $u \approx 170$ cm/sec) than in ideal tubes. Coiling stabilizes "laminar" flow as a result of the secondary flow.

A comparison of Figs. 5 and 6 indicates that h versus u plots are a more sensitive indicator than K versus u curves of the onset of turbulent flow.

In the laminar region the ratio of h values for ideal and coiled tubes increases with increasing velocity. As is evident from Fig. 6 and calculated from eqn. 8, this ratio is about 40 at $u = 120$ cm/sec ($h_{ideal} = 380$ cm and $h_{coil} = 9$ cm, $D = 3.3 \cdot 10^{-5}$ cm^2/sec).

The h versus u and K versus u plots for the 0.25 mm I.D. × 1.5 mm O.D. coiled copper tubes are presented in Fig. 7. The measurements were carried out only up to $u = 250$ cm/sec ($Re = 1060$). Owing to wall roughness, the permeability was lower than the calculated theoretical value of $1.95 \cdot 10^{-5}$ cm^2, even at low velocity; it de-
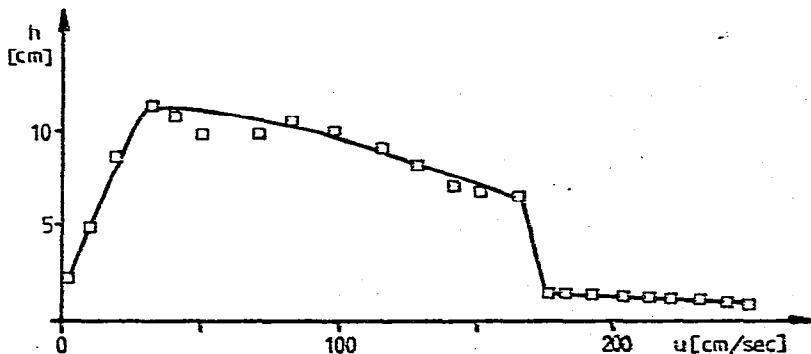

Fig. 6. h versus u curve for a coiled tube (I.D. 1 mm). Conditions as in Fig. 5.

creased with increasing velocity from $1.5 \cdot 10^{-5}$ to $1.0 \cdot 10^{-5}$ cm². It is noteworthy that owing to wall roughness the same permeability ($1.5 \cdot 10^{-5}$ cm²) was found in a straight tube of the same diameter (Fig. 3), although in this instance K remained independent of velocity up to $u = 250$ cm/sec.

The h versus u curve in Fig. 7 is considerably flattened as a result of the secondary flow caused by the coiling. Even though secondary flow also occurs in the straight tube owing to wall roughness, the h value at $u = 250$ cm/sec is 5 times smaller in Fig. 7 than in Fig. 3. These results again indicate that h versus u curves are a considerably more sensitive indicator than K versus u plots of the appearance of secondary flow.
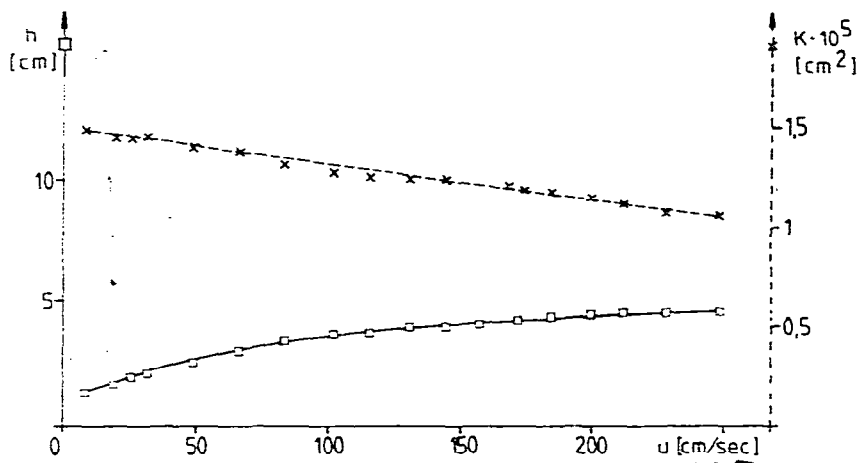

Fig. 7. h versus u (□) and K versus u (×) curves for a coiled tube (I.D. 0.25 mm). Conditions as in Fig. 5, except 0.25 mm I.D. × 1.5 mm O.D.

The shape of the curves obtained with 0.5 mm I.D. × 1.5 mm O.D. coiled copper tubes was similar to that shown in Fig. 7, although because of the larger diameter the h and K values were correspondingly higher[11].

To verify that the method of coiling employed resulted in no changes in the cross-section, measurements were performed on 0.5-mm I.D. tubes with O.D. 1.5 and 3.2 mm. The shapes of the h versus u and K versus u curves for both tubes were very similar[11].

Fig. 8 shows the data for a 0.75 mm I.D. × 2.0 mm O.D. coiled copper tube. Even though $Re = 2300$ was attained at $u = 180$ cm/sec, neither curve indicates the onset of turbulence. In this instance also, secondary flow stabilizes laminar flow and displaces the transition to higher velocities.

The permeability decreases monotonically even at low velocities and at $u = 205$ cm/sec attains about half of the $K_{theo} = d^2/32$.

Band broadening increases to its maximum value ($h = 11$ cm) at $u = 70$ cm/sec and declines slowly to 8 cm at $u = 205$ cm/sec. The relative dispersion continues to decrease with increasing tube diameter as a result of the increased rate of mass transfer brought about by the secondary flow. At $u = 70$ and 150 cm/sec the experimental values for coiled tubes (Fig. 8) are 50 and 150 times smaller, respectively, than those calculated via the Taylor equation (eqn. 8) for ideal tubes where no secondary
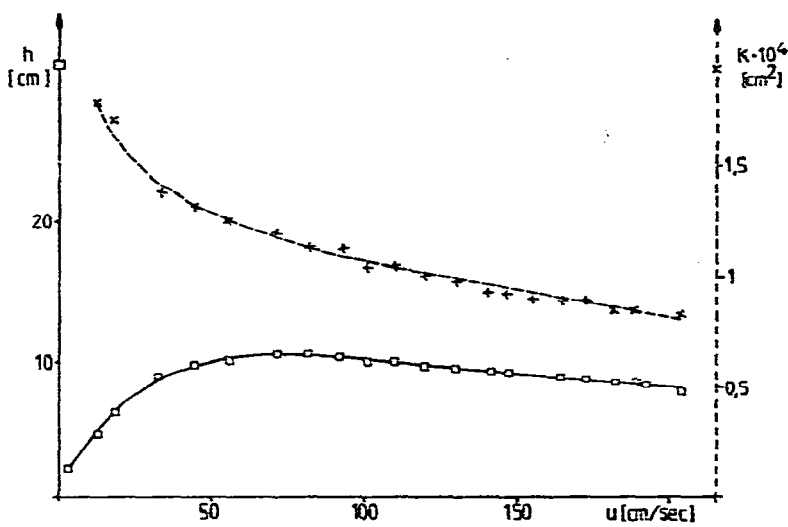
Fig. 8. h versus u ($\square$) and K versus u ($\times$) curves for a coiled tube (I.D. 0.75 mm). Conditions as in Fig. 7, except 0.75 mm I.D. $\times$ 2.0 mm O.D.

flow occurs. Hence, although there is no firm theoretical basis for it, experimentally this factor is found to increase with increasing inner diameter of the open tube. The same coil radius is assumed in this comparison.

The data for the 1.2 mm I.D. $\times$ 2.0 mm O.D. copper tubes (Fig. 9) indicate that the permeability is the same as for ideal tubes ($K_{ideal} = 4.5 \cdot 10^{-4}$ cm^2) at very low velocities. From $u = 10$ cm/sec K decreases monotonically with increasing u and continuously approaches the value for turbulent flow; at $u = 100$ and 140 cm/sec ($Re = 2040$ and 2860), for example, K amounts to 42 and 40 %, respectively of K_{ideal}. These curves show no obvious onset of turbulence. Within the limits of error, these tubes exhibited the same permeability at the corresponding u values as the ideal tubes in the turbulent region.

The dispersion in these tubes increases up to $u = 20$ cm/sec ($h = 11.5$ cm) and passes through a maximum, and the onset of turbulence is indicated distinctly at $u = 140$ cm/sec ($Re = 2860$) by the inconsistency of the h versus u curve. From $h = 4$ cm at the latter velocity, the dispersion decreases to 1.5 cm at $u = 150$ cm/sec and then gradually to 1 cm at 200 cm/sec.

Similar results were also obtained with 1.4 mm I.D. $\times$ 2.0 mm O.D. and 2.0 mm I.D. $\times$ 3.2 mm O.D. coiled copper tubes, as shown in Fig. 9.

To illustrate the experimental difficulties and to point out possible misinterpretations, data for the 4.0 mm I.D. $\times$ 6.0 mm O.D. coiled tubes are presented in Fig. 10. The peaks obtained with a coil diameter of 12 cm for both 10- and 20-m lengths could not be evaluated. Symmetrical peaks were obtained only with an 80-cm coil diameter, but even for the 20-m length (upper curve) the ascending branch c. the h versus u curve could not be determined. Between $u = 5$ cm/sec ($h = 55$ cm) and $u = 40$ cm/sec ($h = 22$ cm) the curve decreases continuously, and turbulence sets in at $u = 45$ cm/sec ($Re = 3060$, $h = 5$ cm). This linear velocity corresponds to a flow-rate of 340 ml/min. The limitations of the pump output prevented measurements at higher
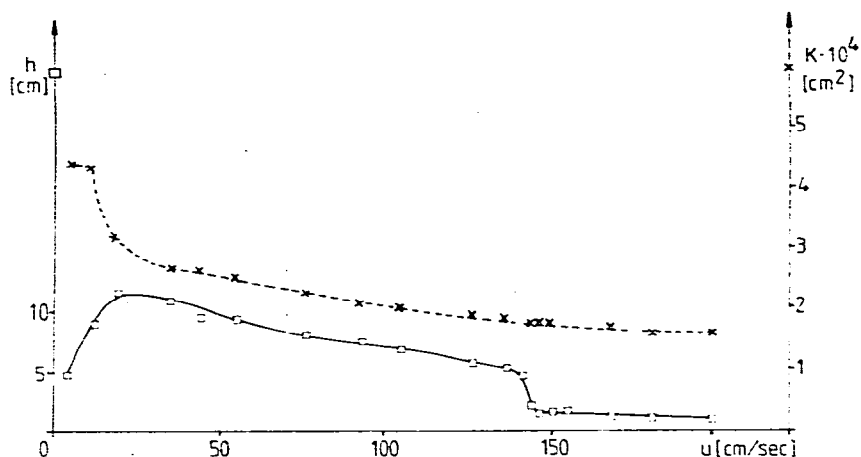
Fig. 9. *h versus u* (□) and *K versus u* (×) curves for a coiled tube (I.D. 1.2 mm). Conditions as in Fig. 7, except 1.2 mm I.D. × 2.0 mm O.D.

velocities. The pressure drop over this column was less than 0.2 bar and could not be measured accurately with the manometer used. Therefore, a *K versus u* curve was not evaluated.

The lower curve in Fig. 10 depicts the data for the 10-m tube (80-cm coil diameter). The inlet and outlet disturbances were obviously appreciable and determined the shape of the curve.

Water as mobile phase

The dispersion of acetone in water was determined in all of the coiled tubes (I.D. 0.25–4.0 mm[11]) as for *n*-heptane. The onset of turbulence in water occurs at
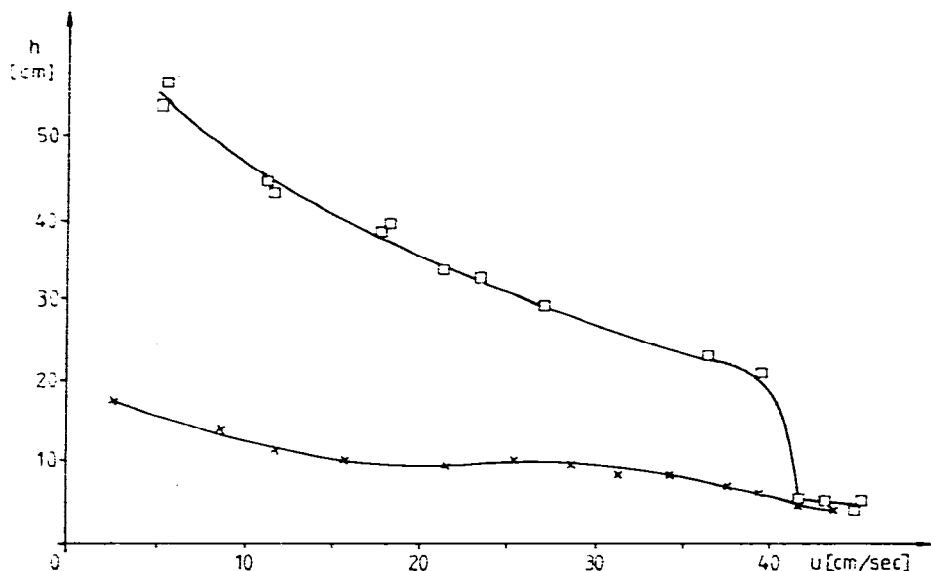

Fig. 10. *h versus u* curve for a coiled tube (I.D. 4 mm). Conditions as in Fig. 5, except coil diameter 80 cm. Column length: □, 20 m; ×, 10 m.

substantially higher velocities because its kinematic viscosity is higher than that of
n-heptane. It is noteworthy, but still unexplainable, that considerably more asym-
metric peaks were obtained that could not be evaluated in comparison with n-heptane.
For this reason, the data for the 1.0 mm I.D. $\times$ 2.0 mm O.D. tube, which were de-
signated as typical in this work, are not shown. To shorten the presentation, only select-
ed results will be discussed, as similarly shaped curves were obtained for both water
and n-heptane at the same Reynold's numbers.

The measurements for the 0.25 mm I.D. $\times$ 1.5 mm O.D. tube (Fig. 11) were
carried out only up to $u = 260$ cm/sec ($Re = 650$). Wall roughness becomes notice-
able as in Fig. 7. With increasing velocity the h values rise monotonically to a plateau
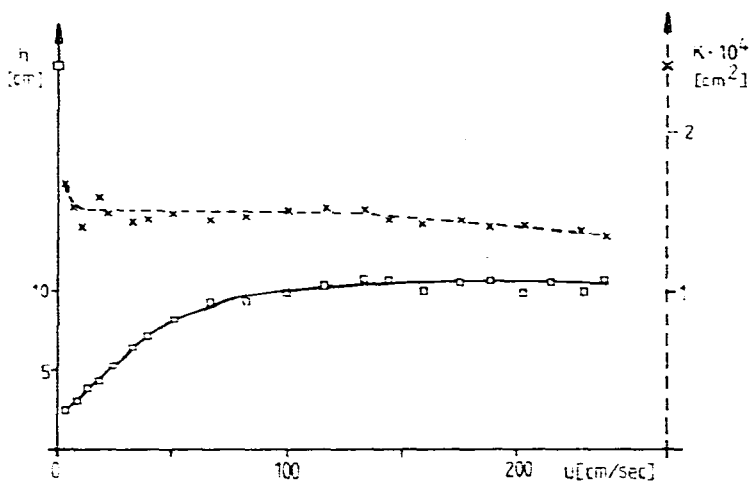from $u = 50$ cm/sec ($h = 9.5$ cm) to $u = 240$ cm/sec ($h = 11$ cm) and then decline
slowly.

Fig. 11. h versus u ($\square$) and K versus u ($\times$) curves for a coiled tube (I.D. 0.25 mm). Copper tube
(0.25 mm I.D. $\times$ 1.5 mm O.D.), $L = 10$ m. Coil diameter: 12 cm. Eluent, water; sample, acetone;
room temperature.

Compared with that of ideal tubes, the permeability was about 10% lower at
$u = 5$ cm/sec and 25% lower from $u = 10$ cm/sec upwards. From 150 cm/sec the
permeability decreased gradually.

For the 0.75 mm I.D. $\times$ 2.0 mm O.D. tubes (Fig. 12), h reaches its maximum
value of 26 cm at $u = 40$ cm/sec and decreases to 17.5 cm at $u = 122$ cm/sec. From
this velocity to 300 cm/sec the peaks are too asymmetric for evaluation. The onset of
turbulence occurs between 330 and 365 cm/sec ($Re = 2480$ and 2730) and the h
values drop to 2.2 cm. Hence, laminar flow in coiled tubes is stabilized in water also
and turbulence is displaced to higher Reynold's numbers. The permeability decreases
continuously with increasing velocity to the values in turbulent flow.

Fig. 13 contains the results for 1.2-mm I.D. tubes. The h versus u curve passes
through a maximum at $u = 25$ cm/sec ($h = 31.5$ cm) and then decreases monotoni-
cally to $h = 6$ cm at $u = 215$ cm/sec ($Re = 2580$). Turbulence sets in at $u = 263$
cm/sec ($Re = 3160$) and h is 1.5 cm. The permeability decreases continuously with
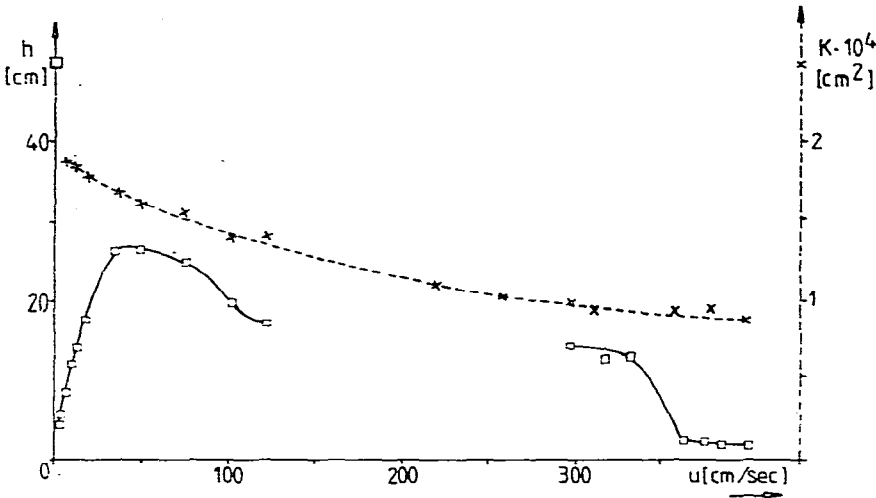increasing velocity and the onset of turbulence is not obvious from this curve.

Fig. 12. *h versus u* (□) and *K versus u* (×) curves for a coiled tube (I.D. 0.75 mm). Conditions as in Fig. 11, except 0.75 mm I.D. × 2.0 mm O.D.
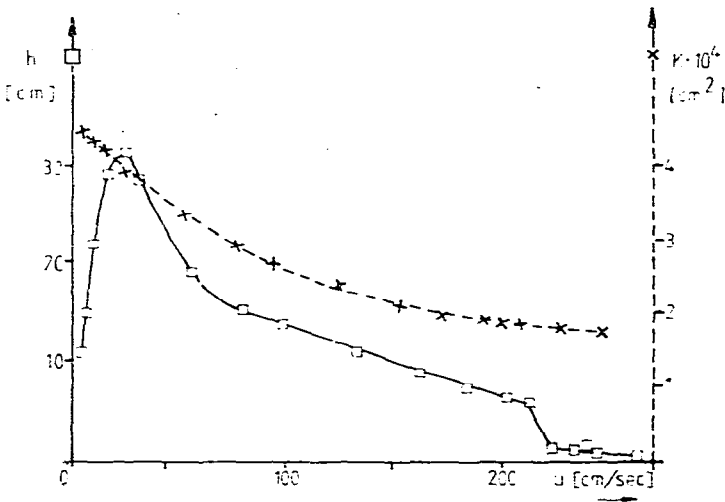

Fig. 13. *h versus u* (□) and *K versus u* (×) curves for a coiled tube (I.D. 1.2 mm). Conditions as in Fig. 11, except 1.2 mm I.D. × 2.0 mm O.D.

The shapes of the *h versus u* and *K versus u* curves for 1.4-, 2.0- and 4.0-mm I.D. tubes are similar to that shown in Fig. 13. Thick- and thin-walled tubes with the same inner diameter display no appreciable differences in their *h versus u* or *K versus u* curves.

ACKNOWLEDGEMENTS

SYMBOLS

d (cm)	inner diameter of the open tube
D (cm^2/sec)	interdiffusion coefficient of the sample in the mobile phase
D_{calc} (cm^2/sec)	D calculated via eqn. 8
D_{dyn} (cm^2/sec)	defined in eqn. 5
F (cm^3/sec)	flow-rate of the eluent
h (cm)	height equivalent to a theoretical plate or relative band broadening
h_{turb} (cm)	h at u_{turb}
K (cm^2)	specific permeability as defined in eqn. 1
K_{theo} (cm^2)	$= d^2/32$
k'	$= (t_R - t_0)/t_0 =$ capacity ratio
L (cm)	column length
L_e (cm)	length of the inlet (or outlet) turbulence as defined in eqn. 3 or 10
n	number of theoretical plates
ΔP (bar)	pressure drop over the column
r (cm)	radius of the open tube
Re	Reynold's number, as defined in eqn. 4
Re_{crit}	critical Reynold's number
t (sec)	time
t_0 (sec)	retention time of an inert sample
t_R (sec)	retention time of a retarded peak
u (cm/sec)	cross-section averaged linear velocity of the mobile phase
u_{crit} (cm/sec)	minimum velocity in the turbulent region
u_{max} (cm/sec)	maximum velocity of the mobile phase
u_{sym} (cm/sec)	maximum linear velocity in the laminar region at which symmetrical peaks are obtained
u_{turb}	u at incipient turbulence
w (sec)	peak width
η (poise)	dynamic viscosity
ϱ (g/cm^3)	density
v (stokes)	$= \eta/\varrho$ kinematic viscosity
σ (cm)	standard deviation of a Gaussian curve

REFERENCES

1 M. J. E. Golay, in D. H. Desty (Editor), *Gas Chromatography 1958*, Butterworths, London, 1958, p. 36.
2 K. Hofmann, *Diplomarbeit*, Frankfurt/Main, 1966.
3 K. F. Gütlich, *Ph.D. Thesis*, Frankfurt/Main, 1970.
4 I. Halász, H. O. Gerlach, A. Kroneisen and P. Walkling, *Z. Anal. Chem.*, 234 (1968) 97.
5 P. Walkling, *Ph.D. Thesis*, Frankfurt/Main, 1968.
6 I. Halász, H. O. Gerlach, K. F. Gütlich and P. Walkling, *Ger. Pat.*, 1,675,313; *U.S.Pat.*, 3,820,660; *Brit.Pat.*, 1,220,552 (1968).
7 I. Halász and P. Walkling, *Ber. Bunsenges. Phys. Chem.*, 74 (1970) 66.
8 G. Deininger and I. Halász, *J. Chromatogr. Sci.*, 8 (1970) 499.
9 I. Halász in J. J. Kirkland (Editor), *Modern Practice of Liquid Chromatography*, Wiley, New York, 1971, p. 325.

10 G. Deininger, *Ber. Bunsenges. Phys. Chem.*, 77 (1973) 145.
11 K. Hofmann, *Ph.D. Thesis*, Saarbrücken, 1975.
12 M. Martin, G. Blu and G. Guiochon, *J. Chromatogr. Sci.*, 11 (1973) 641.
13 G. Hagen, *Poggendorfs Ann.*, 4b (1839) 423.
14 J. L. M. Poiseuille, *C.R. Acad. Sci.*, (1840) 11; (1841) 12; *Mem. Savants Etrang.*, (1846) 9.
15 F. Bosnjakovic, *Technische Thermodynamik, Teil I*, Th. Steinkopf, Dresden, 6th ed., 1972, pp. 468ff.
16 G. I. Taylor, *Proc. Roy. Soc. London*, A225 (1954) 473.
17 R. Aris, *Proc. Roy. Soc. London*, A235 (1956) 67.
18 A. Einstein, *Ann. Phys.*, 17 (1905) 549.
19 L. Prandtl, *Führer durch die Strömungslehre*, Vieweg, Braunschweig, 6th ed., 1965, pp. 196ff.
20 W. R. Dean, *Phil. Mag.*, 7/4 (1927) 208.
21 W. R. Dean, *Phil. Mag.*, 7/5 (1928) 67.
22 I. Halász, A. Kroneisen, H. O. Gerlach and P. Walkling, *Z. Anal. Chem.*, 234 (1968) 81.
23 G. Deininger and I. Halász, *J. Chromatogr.*, 60 (1971) 65.
24 G. I. Taylor, *Proc. Roy. Soc. London*, A223 (1954) 446.
25 L. Prandtl, *Z. Angew. Math. Mech.*, 5 (1925) 136.
26 L. Prandtl, *Phys. Z.*, 29 (1925) 487.
27 C. R. Wilke and P. Chang, *Amer. Inst. Chem. Ing.*, 261 (1955) J 1.